

Short-Term Advanced Warning from Some Large Earthquakes

Indra N. Gupta, B.K. Rastogi* and Robert A. Wagner

Array Information Technology, Greenbelt, Maryland

*Former Director General, Institute of Seismological Research, Gandhinagar, India

*Corresponding Author: bkrastogi12@gmail.com

ABSTRACT

Several recent studies have identified short-term precursory activity before large earthquakes. Ambient seismic noise with spectral peaks at about 0.07 Hz and 0.2 Hz, due to primary and secondary microseisms, respectively, is observed everywhere at stations on hard basement rock. We examined pre-earthquake ambient seismic noise from four large earthquakes recorded at several three-component stations. Spectral characteristics of seismic noise within a narrow frequency range, which includes the larger-amplitude secondary spectral peak frequency, are found to be significantly altered by pre-earthquake activity when monitored by stations near the earthquake epicenter. For the M6 Nevada earthquake of 21 February 2008, spectral ratios of transverse/radial component or T/R observed at two recording stations along nearly orthogonal directions with respect to the epicenter suggest that the pre-seismic energy consists of the lowest frequencies up to about 0.2 Hz and increases in strength as it approaches the earthquake origin time. Moreover, the differences in T/R at the two stations are found to be in agreement with regional tectonics, therefore suggesting a mechanism of accelerating movement on pre-existing faults in the region. Analysis of several hours of observed pre-earthquake noise from four large earthquakes, obtained by converting observed data to particle displacement, show the low frequency amplitudes to increase in strength as the earthquake origin time approaches. Moreover, the advanced warning time appears to depend on earthquake magnitude; larger warning times for larger events. Our study appears to provide a method for obtaining advanced warning of a few hours or more before at least some impending large earthquakes.

Key Words: Advanced Warning, Short-term precursory activity, Ambient seismic noise, particle displacement.

INTRODUCTION

Several large earthquakes from all over the world have shown short duration precursory activity. A few examples are the 2011 M 9 Tohoku-oki earthquake (Sato et al., 2013; Uchida et al., 2016), the 2014 Iquique, Chile, Mw 8.2 Earthquake (Kato et al., 2016), and the 2004 Parkfield earthquake (Shelly, 2009). Similarly, in their study of the 1999 Mw 7.6 Izmit earthquake (Bouchon et al., 2011), the event was "preceded for 44 minutes by a phase of slow slip" but also "increased low frequency seismic noise". Although all these are after-the-fact indications, they do provide hope that short-term advanced warning should be possible.

The main feature of ambient noise spectra commonly observed at recording stations on hard rock are two peaks, the main peak is usually at about 0.2 Hz and the smaller peak at about 0.07 Hz and both peaks are due to ocean waves (Aki and Richards, 2009). Recently, Tian and Ritzwoller (2015) found that physical mechanisms and source locations of these primary and secondary microseisms are different. Gupta (1965) demonstrated that a significant fraction of the ambient short-period seismic noise at a given site may be attributed to stationary P waves with spectral characteristics strongly dependent on the geological structure underlying the recording station. In this study, we examine how the spectral characteristics

of ambient noise, especially its dominant peak at about 0.2 Hz, are impacted by pre-earthquake activity.

We analyzed pre-earthquake good-quality three-component continuous data from four large earthquakes, for several segments of time, including those starting several hours prior to the earthquake origin time and ending just before the first P from the event. These four earthquakes are (1) Nevada earthquake, 21 February 2008, epicenter at 41.15°N, 14.87°W, magnitude 6, depth 6.7 km.; (2) Southern California earthquake, 12 June 2005, epicenter at 33.53°N, 116.58°W, magnitude 5.2, depth 14.2 km.; (3) Craig, Alaska earthquake, 5 January 2013, epicenter 55.4°N, 134.7°W, magnitude 7.5, depth 10 km; and (4) Hindu Kush Earthquake, 26 October 2015, epicenter 36.5°N, 70.4°E, magnitude 7.5, depth 213 km.

ANALYSIS OF PRE-EARTHQUAKE SEISMIC NOISE FOR AN EARTHQUAKE IN NEVADA

We first analyzed pre-earthquake seismic noise from the Nevada 2008 event (Figure 1) by retrieving continuous ambient noise data recorded at several stations. Several hours' long samples of noise at three different times spanning a year, including a segment ending just a few seconds before the first P from the earthquake, were selected. For each segment, the horizontal components were

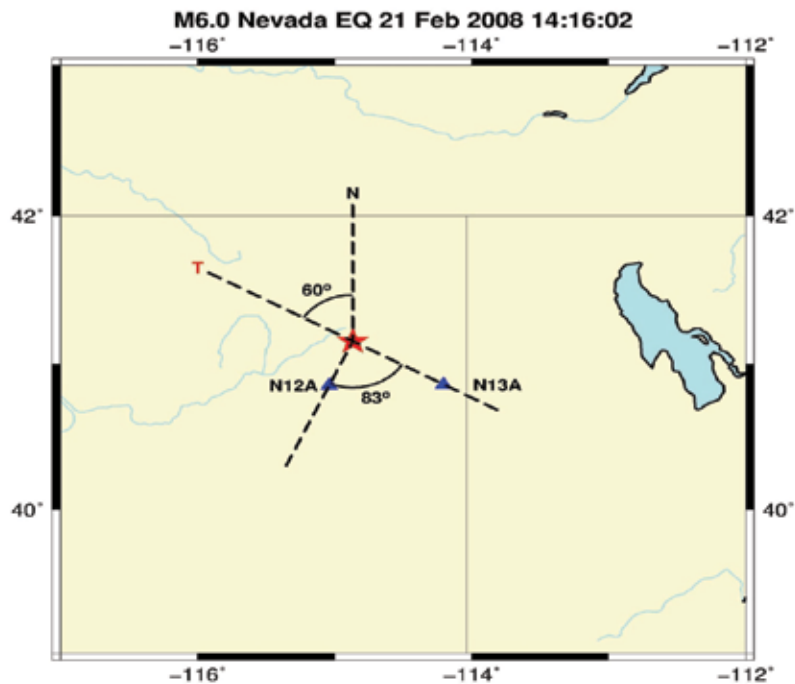


Figure 1. Epicentral location of Magnitude 6 earthquake in Nevada with its epicenter (red star) and two stations N12A and N13A at epicentral distances of 36 and 65 km, respectively. The two stations are nearly along orthogonal directions with respect to the epicenter and the known direction of T axis (N 60° W) coincides with the azimuthal direction of N13A.

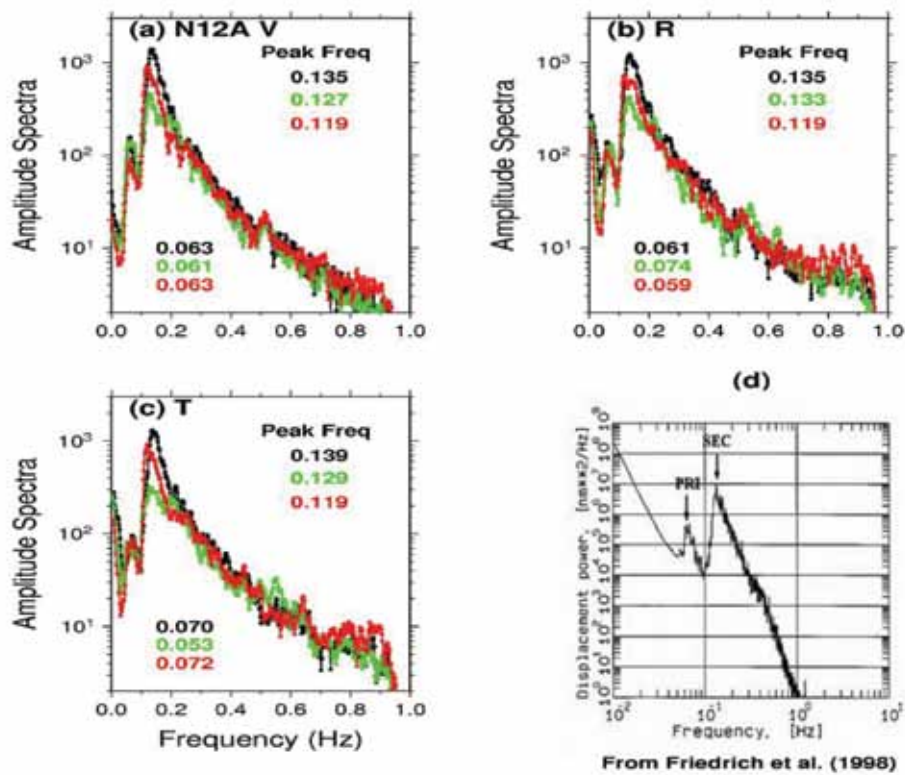


Figure 2. Spectra of (a) vertical (V), (b) radial (R) and (c) transverse (T) components of seismic noise at three different times preceding the earthquake: one-year before (black), one-month-before (green) and just-before (red). Each of the three sets of spectra shows two low-frequency peaks similar to those in (d) for V component at the Grafenberg array. The higher frequency peak values show a shift to lower values as the earthquake origin time approaches.

rotated into T and R components, based on the known epicenter. For the nearest station, N12A, spectra of vertical (V), radial (R) and transverse (T) components of 2048 sec long samples of noise at three different times preceding the earthquake: one-year-before (black), one-month-before (green) and just-before (red) are shown in Figure 2 (a), (b) and (c). These three figures used 2048 sec segments with sample rate of 2 samples per sec (decimated by 20) so that the Nyquist frequency is 1.0 Hz. An average of four spectral windows, each 512 seconds long, was used in order to show more detail at the lower frequencies. The three sets of spectra appear to be fairly similar with two prominent low frequency peaks for each component. It is interesting to note that two similar low-frequency peaks, considered to be due to primary and secondary microseisms, were observed in a study of ocean-generated seismic noise (vertical component) recorded at the Gräfenberg array by Friedrich et al., (1998), reproduced in Figure 2(d). The agreement between the spectral peak values in their study with ours for one-year before (black) is indeed remarkable. Apparent lack of agreement at the lowest frequencies is because of the fact that Figure 2(d) is in displacement whereas station N12A is a particle velocity instrument. For the three sets of spectra in Figures 2(a), (b) and (c), the larger amplitude spectral peaks within 0.1-0.2 Hz show a small systematic decrease in their frequency values for just-before (red) and one-month-before (green) segments of noise as compared to those for one-year-before (black).

Using data from both N12A and N13A, four spectral ratios, T/R, each based on averaging 5 windows, each 102.4 sec long for a total segment length of 512 seconds are shown in Figure 3(a). For recordings at the station N12A, T/R for the segment just-before the first P is shown in red whereas that for the one-year before segment is shown in black. Similar spectral ratios from N13A are shown in blue for the just-before segment and in dashed black for the one-year before segment. A comparison of the two just-before segments for N12A (red) and for N13A (blue) shows significant differences, including opposite trends for the lowest frequencies of up to at least about 0.2 Hz. The most likely reason for this is the large difference of 83 degrees in their epicenter-to-station azimuthal directions, which makes the transverse direction for one recording station nearly the same as the radial direction for the other station. Similar results, obtained by averaging 20 windows, each 102.4 sec long, for a total segment length of 2048 seconds, are shown in Figure 3(b). Results regarding opposite trends for the lowest frequencies at the two stations are similar but T/R amplitudes are smaller than those for the shorter noise segments, suggesting acceleration with amplitudes increasing with time up to the earthquake origin time.

Nevada is known to be a region of active tectonic processes with the direction of minimum principal stress to be about N 60° W (e.g. VanWormer and Ryall, 1980).

This happens to be the same as the azimuthal direction of N13A with respect to the epicenter. This means that the significant differences in the spectral ratios at the two stations (Figure 3) are fully consistent with regional tectonics and therefore indicate that pre-existing faults in the epicentral region start accelerating, accompanied by radiation of low frequency seismic waves, prior to the earthquake occurrence.

ADVANCED WARNING BASED ON BROADBAND DISPLACEMENT LOW FREQUENCY SPECTRA

We next analyze low frequency displacement spectra of pre-seismic noise by converting the observed spectral amplitudes from particle velocity to displacement. For this, we first analyzed pre-event noise from the Nevada earthquake recorded at two stations N12A and N13A and the results are shown in Figures 4 and 5. For each figure, we start with obtaining spectra of consecutive 256 sec windows, convert the observed spectral amplitudes to displacement and compute mean log amplitude within a narrow frequency range, such as 0.1 to 0.2 Hz, which includes the secondary peak frequency in ambient seismic noise. These mean values are plotted versus 120 time windows, covering a period of 8.4 hours of continuous pre-earthquake noise ending just before the event origin time, for (a) V, (b) R and (c) T components. The first half of these 120 windows is shown in green color and the other half in red. Mean values for the entire duration, after dividing it into 8 segments S1, S2, S3,.....S8, each consisting of 15 windows, are shown by superimposed black straight lines. For each component, the difference between the mean amplitude values of the last segment S8 and the first segment S1, $S8 - S1$ is indicated along with its value as a percentage increase. Both Figures 4 and 5 indicate almost systematic and significant pre-earthquake increase in amplitudes on all three components and the increase during the last four hours (red) appears to be larger than that during the first 4 hours (green).

Similar analysis of data for the Southern California earthquake of 12 June 2005 recorded at SND led to results shown in Figure 6. Note that the mean values, shown by superimposed black straight lines, again show systematic general increase with time but the increase is much smaller than in Figures 4 and 5. Most likely reason is the much smaller magnitude (M 5.2) of this earthquake as compared to the Nevada event (M 6).

Figure 7 shows results for the Craig, Alaska earthquake of 5 January 2013 recorded at CRAG at an epicentral distance of 97 km. Here the mean values show a large and almost steady increase over the entire duration of 120 windows, suggesting an advanced warning time of much longer duration.

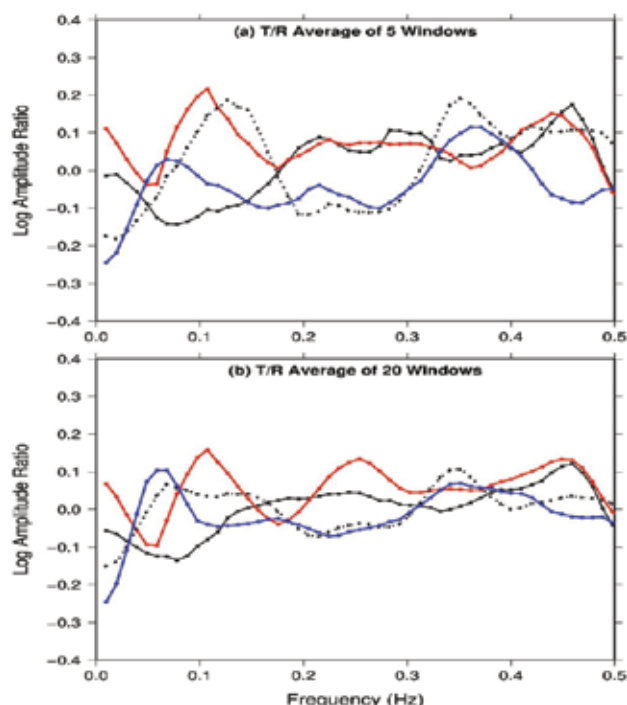


Figure 3. (a) Spectral ratios T/R for stations N12A and N13A for noise time segments of 512 sec each. For N12A, T/R for the segment just-before the first P is shown in red whereas that for the one-year before is shown in black. Similar spectral ratios from N13A are shown in blue and dashed black. A comparison of the two T/R for just-before segments for N12A (red) and for N13A (blue) shows opposite trends for the lowest frequencies of up to about 0.2 Hz. (b) Similar results for segment lengths of 2048 seconds also show opposite trends for the lowest frequencies at the two stations but T/R amplitudes are smaller than those in Figure 3 (a), suggesting acceleration with amplitudes increasing with time up to the earthquake origin time.

Results from the Hindu Kush earthquake of 26 October 2015 recorded at KBL are shown in Figure 8. Similar to the results for Craig, Alaska earthquake, there is steady increase in amplitude over the entire duration of over 12 hours. It seems therefore that for both these two M7.5 earthquakes, the increase in Mean Amplitude may have started earlier than 8 hours before the earthquake. Note that the pre-earthquake low frequency signals from these two large magnitude earthquakes are strong enough to be easily observed at large distances of 97 and even 250 km. Observation of strong precursory signals at an epicentral distance of 250 km for the Hindu Kush earthquake does seem hard to believe until one considers its large 213 km hypocentral depth. At this depth in the mantle, the S wave velocity is about 5 km/sec so that for a frequency of 0.1 Hz the wavelength is about 50 km and an epicentral distance of 250 km implies a distance of only 5 wavelengths.

The above results from four large earthquakes demonstrate that the pre-earthquake source consists of a

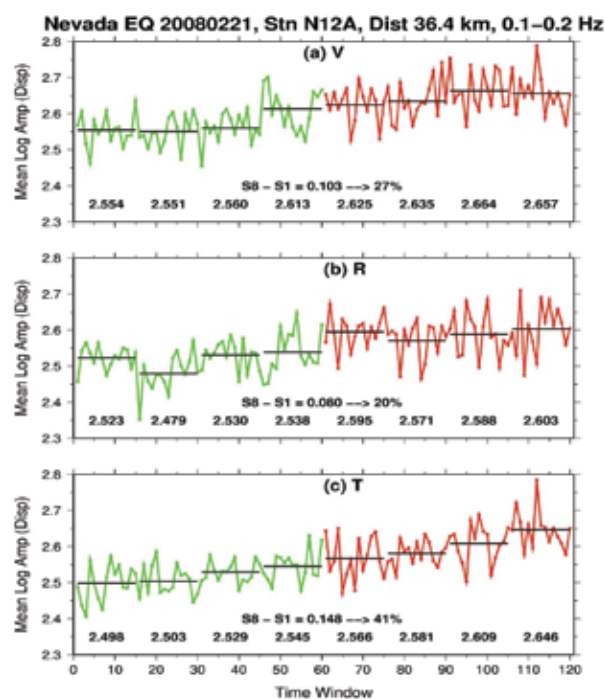


Figure 4. Mean log amplitude (displacement) for Nevada earthquake recorded at N12A vs 120 time windows, covering a period of 8.4 hours of continuous pre-earthquake noise ending just before the origin time, for (a) V (b) R and (c) T components, with the first half shown in green color and the other half in red. Mean values for the entire duration, after dividing into 8 segments S1, S2, S3,.....S8, each consisting of 15 windows, are shown by superimposed black straight lines. For each component, the difference between the last segment, S8 and the first segment S1, $S8 - S1$ is indicated along with its value as a percentage increase. As indicated by the mean values for the eight segments, this precursory signal progressively gains strength as the earthquake origin time approaches.

broadband displacement low frequency spectrum increasing in strength as the earthquake origin time approaches. Our observations indicate that such a signal, emanating from the pre-earthquake, gets superimposed on the ambient seismic noise spectra at recording stations. Moreover, a comparison of results for the four earthquakes suggests dependence of advanced warning time on magnitude of the earthquake, with larger warning time for larger events.

BACKGROUND AND DISCUSSION OF RESULTS

A short description of relevant studies of short-term pre-seismic phenomena follows. Dieterich (1978) proposed that “pre-seismic fault slip takes place in two stages. The first stage consists of the long-term stable propagation of slip along the fault. The second stage is the shorter interval of accelerated slip that culminates in seismic instability.” A review article by Chelidze and Matcharashvili (2007) contends that whereas long term prediction may never be

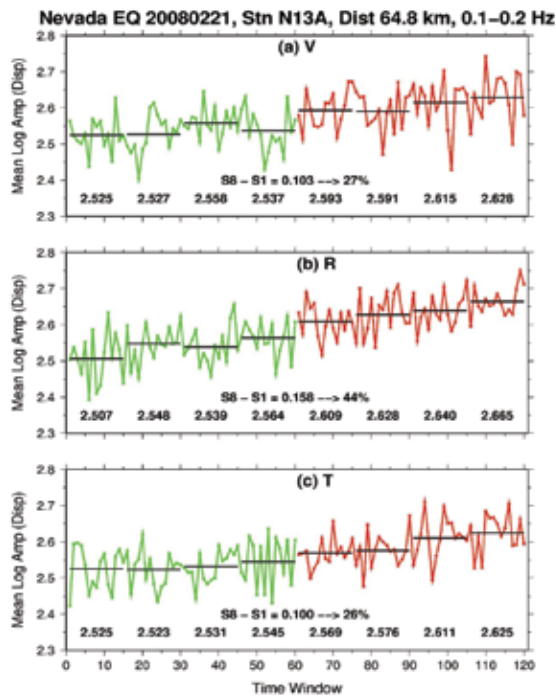


Figure 5. Similar to Figure 4 but for N13A. Again, the mean values, shown by superimposed black straight lines, indicate significant premonitory increase with time, more so during the last half (red).

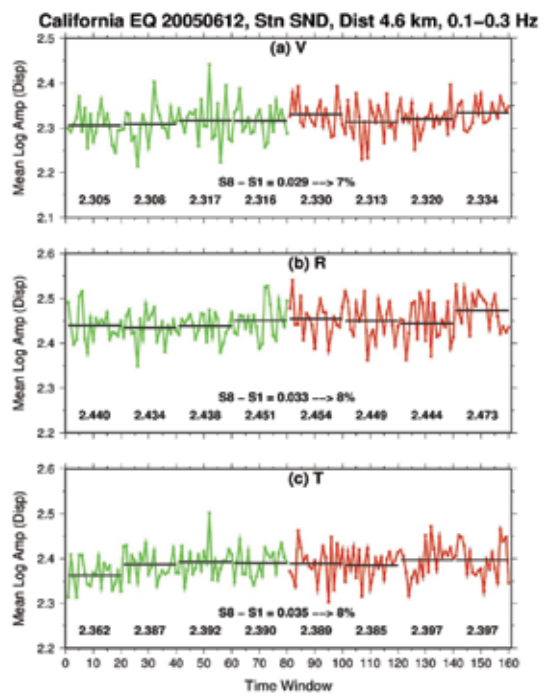


Figure 6. Similar to Figure 4 but for the Southern California earthquake recorded at SND. The mean values, shown by superimposed black straight lines, do indicate overall increase with time but much smaller than in Figures 4 and 5. The most likely reason is much smaller magnitude ($M 5.2$) of this earthquake as compared to the Nevada event ($M 6.0$).

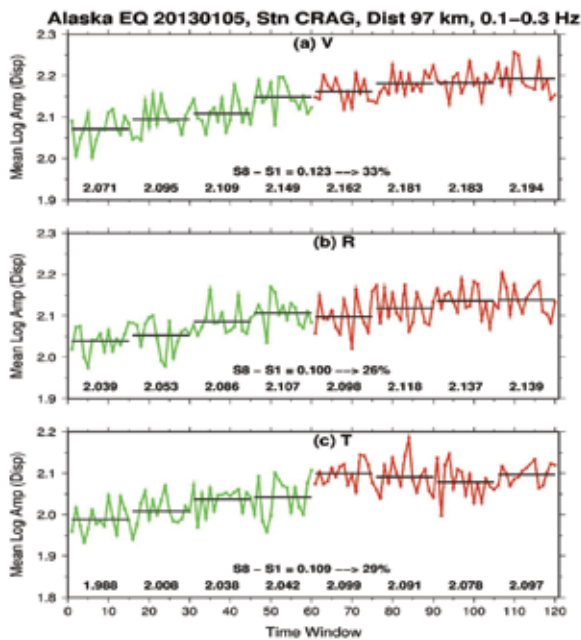


Figure 7. Similar to Figure 4 but for the Alaska earthquake recorded at CRAG. The mean values not only indicate strong increase with time but also the increase in Mean Amplitude may have started earlier than 8 hours before the earthquake.

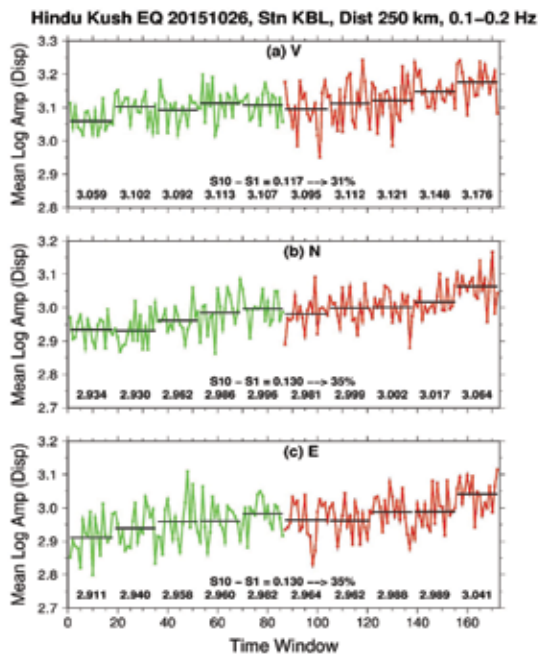


Figure 8. Similar to Figure 4 but for the Hindu Kush earthquake recorded at KBL based on over 18 hours of data. As for the Alaska earthquake (Figure 7), the mean values not only indicate strong increase with time but also the increase in Mean Amplitude may have started earlier than 8 hours before the earthquake.

possible, a limited time interval before a large earthquake should be predictable." Laboratory and theoretical studies suggest that earthquakes may be preceded by a phase of developing slip stability in which the fault begins to slip slowly before accelerating to dynamic rupture (Bouchon et al., 2011). A recent study by Uchida et al., (2016) found slow slip acceleration to precede the 2011 M 9 Tohoku-oki earthquake for which the slow slip began accelerating a few days before the main shock.

According to Marsan et al., (2015), "Researchers now understand that faults do not just remain totally locked between earthquakes (rapid slip events that efficiently radiate seismic waves) or creep steadily and slowly (without radiating). Instead, faults may be better described as patchworks of slip behaviors spanning a complete spectrum between these end members". Our results, suggesting that pre-existing faults in the epicentral region start accelerating accompanied by radiation of low frequency seismic waves prior to the earthquake occurrence, are therefore fully consistent with all these authors.

Analysis of low frequency data from four large earthquakes (Figures 4, 5, 6, 7 and 8) indicate that a broadband displacement low frequency signal emanates from the pre-earthquake source and gets superimposed on the existing ambient seismic noise and this signal becomes progressively stronger as the origin time approaches. These results may therefore be used to obtain advanced warning of a few hours or more before a large earthquake.

CONCLUSION

Our results suggest that the pre-earthquake fault slip before a large earthquake is associated with a broadband displacement low frequency signal, starting rather gradually a few hours before the earthquake and increasing in strength with time. This mechanism seems to be in agreement with several recent studies of pre-earthquake phenomena. Monitoring these temporal variations in mean amplitude over a narrow frequency band (which included the secondary spectral peak in ambient seismic noise) displayed an almost continuous temporal increase lasting up to the earthquake origin time. Our analysis of data from four large earthquakes provides remarkably consistent results leading to a relative simple methodology for obtaining warning of four hours or better before at least some large earthquakes.

ACKNOWLEDGMENTS

We sincerely appreciate numerous helpful suggestions from Professor Paul Richards and Dr. David Schaff, both at Columbia University. We are also most grateful to

Dr. Robert Blandford for his encouragement and numerous suggestions. We also thank Dr. H.M. Iyer for his review. Thanks are due to Shri D.N. Avasthi and Dr. P.R.Reddy for the efforts to publish this article in JIGU.

Compliance with Ethical Standards

The authors declare that they have no conflict of interest and adhere to copyright norms.

REFERENCES

- Aki, K., and P.G., Richards, 2009. Ambient seismic noise, in *Quantitative Seismology*, pp: 616-617.
- Bouchon, M., Karabulut, H., Aktar, M., Ozalaybey, S., Schmittbuhl J., and Bouin, M., 2011. Extended nucleation of the 1999 Mw 7.6 Izmit earthquake, *Science*, v. 331, pp: 877-880.
- Chelidze, T., and Matcharashvili, T., 2007. Complexity of seismic process; measuring and applications - A review, *Tectonophysics*, v.431, pp: 49-60.
- Dieterich, J. H., 1978. Preseismic Fault Slip and Earthquake Prediction, *Jour. Geophys. Res.*, v.83, pp: 3940-3947.
- Friedrich, A., Krüger, F., and Klinge, K., 1998. Ocean-generated microseismic noise located with the Gräfenberg array, *Journal of Seismology*, v.2, no.1, pp: 47-64.
- Gupta, I. N., 1965. Standing-wave phenomena in short-period seismic noise, *Geophysics*, v.30, pp: 1179-1186.
- Kato, A J., Fukuda, T., and Nakagawa, S., 2016. Accelerated nucleation of the 2014 Iquique, Chile, Mw 8.2 earthquake. *Sci. Rep.* v.6, pp: 24792.
- Marsan, D., Gombert, J., and Bouchon, M., 2015. Exploring earthquakes, slow slip, and triggering, *Eos*, 96, 20 March 2015.
- Sato, T., Hiratsuka, S., and Mori, J., 2013. Precursory seismic activity surrounding the high-slip patches of the 2011 Mw 9.0 Tohoku-Oki earthquake, *Bull. Seism. Soc. Am.* v.103, pp: 3104-3114.
- Shelly, D. R., 2009. Possible deep fault slip preceding the 2004 Parkfield earthquake, inferred from detailed observations of tectonic tremor, *Geophysical Res. Lett.* v.36, pp: L17318.
- Tian, Y., and Ritzwoller, M. H., 2015. Directionality of ambient noise on the Juan de Fuca plate: implications for source locations of the primary and secondary microseisms, *Geophysical Journal International*, v.201, pp: 429-443.
- Uchida, N., Linuma, T., Nadeau, M.H., Burgmann, R., and Hino, R., 2016. Periodic slow slip triggers megathrust zone earthquakes in northeastern Japan, *Science*, pp: 488-492.
- VanWormer, J. D., and Ryall, A., 1980. Sierra Nevada-Great Basin boundary zone: earthquake hazard related to structure, active tectonic processes, and anomalous patterns of earthquake occurrence.

Received on: 13.1.18; Accepted on: 19.1.18.